

Research on rockburst proneness evaluation method of deep underground engineering based on multi-parameter criterion

Feiyue Sun^a, Wenlong Wu^b, Zhijia Wang^{c*}, Zhihai Liu^d, Zhuang Shao^d

^a School of Civil Engineering, Henan Polytechnic University, Jiaozuo 454000, Henan, China

^b School of Civil and Traffic Engineering, Henan University of Urban Construction, Pingdingshan, 467001, Henan, China

^c School of Business Administration, Henan Polytechnic University, Jiaozuo 454000, Henan, China

^d China Construction Seventh Engineering Division Co., Ltd., Zhengzhou 450000, Henan, China

*Correspondence author: wangzhijiaww@163.com

ABSTRACT: The study of rockburst criterion is the key to predict the occurrence of rockburst. Based on the energy principle, a new multi-parameter rockburst criterion (RPC) were established. The accuracy and applicability of some typical rockburst engineering examples in China were verified by using some classical rockburst criteria and the newly proposed RPC. The research results show that: RPC comprehensively considers the various stress states of the surrounding rock mass unit, and reflects the integrity factors, mechanical factors, brittleness factors and energy storage factors in the process of rockburst inoculation. Three rockburst classification thresholds (2, 11 and 110) for four grades of none, weak, moderate and severe rockburst were proposed. The prediction and evaluation of rockburst by RPC is basically consistent with the actual situation of rockburst, which can better reflect the overall trend of rockburst failure in deep tunnels.

KEYWORDS: Deep underground engineering; Rockburst proneness; multi-parameter rockburst criterion; Rockburst classification; Numerical simulation.

1 INTRODUCTION

Since the first rockburst occurred in the South Stafford tin mine in the United Kingdom in 1738, many countries and regions have experienced rockburst disasters worldwide, such as South Africa, India, Japan, the United States, France, Switzerland, etc. (Feng et al. 2012, Ma et al. 2015, Wei et al. 2020). The earliest recorded coal-burst in China occurred in the Shengli Coal Mine of Fushun in 1933 (Zhang and Fu, 2008). After that, rockburst frequently occurred in traffic tunnels, hydraulic tunnels and other underground cavern projects in China. Rockburst is a dynamic instability phenomenon of sudden burst caused by the instantaneous release of elastic deformation energy accumulated in rock mass in the process of underground engineering excavation, which is often accompanied by rock ejection or throwing, strong vibration, huge sound and air waves, etc. (Feng et al. 2019). Rockburst has strong suddenness, locality, concealment and harmfulness, which greatly threatens the safety of on-site construction personnel and mechanical equipment and brings serious challenges to the design and construction of deep engineering (Roohollah and Abbas, 2018). For example, during the construction of the Jinping II hydropower station in China, different levels of rockbursts occurred; in 2009, a severe rockburst occurred during the excavation of the drainage tunnel caused a serious accident, which caused the

TBM excavation equipment to be buried and the 28 m support system along the axis of the cavern was destroyed (Feng et al. 2012). Therefore, with the vigorous development of deep underground engineering construction in the world, it is urgent to continuously study the mechanism of rockburst, accurately grasp the law of rockburst inoculation and evolution and the proneness of rockburst occurrence, and accurately predict the strength of rockburst activities. This is of great theoretical significance and engineering application value to ensure the safety and healthy development of underground engineering construction.

The rock mechanics workers and engineering technicians at home and abroad have carried out in-depth research on rockburst criterion and rockburst classification from theoretical analysis, numerical simulation, field monitoring and test under the guidance of deep rock mass mechanics and nonlinear dynamic science theory and put forward corresponding prediction and evaluation indexes based on their respective assumptions. In theoretical research, many experts and scholars have proposed dozens of classical rockburst criteria and intensity classification successively, such as Barton criterion, Turchaninov criterion, Russenes criterion, Kidybinski energy criterion, Hoek criterion, Erlangshan highway tunnel criterion, Gu-Tao criterion and Motycaka energy ratio method, etc. (Barton et al. 1974; Russenes 1974; John et al. 1979;

Kidybinnski 1981; Hoek et al. 1997; Xu et al. 1999; Gu et al. 2002; Zhang et al. 2017). In the field monitoring research, scholars have achieved some fruitful research results, such as microseismic monitoring method, acoustic emission monitoring method, microgravity method, acoustic wave detection method, infrared thermal imaging method and so on (Wu 1993; Chen et al. 2010; Zhang et al. 2012; Zhang et al. 2018; Zhang et al. 2020). In the experimental research, Karchevsky (2017) determined a calculating quantity algorithm and took this algorithm as a standard to distinguish the possibility of rock fracture. Li et al. (2018) established failure criterion of rock strength based on energy mutation. Li et al. (2019) put forward a rockburst dynamic criterion based on dynamic and static energy index. Gong et al. (2020) advanced a rockburst proneness classification standard based on the failure results and phenomena of rock samples tested in laboratory tests. Wu et al. (2020) proposed the classification prediction method of rockburst intensity. With the rapid development of computer technology, numerical analysis method emerges as the times require and becomes more and more perfect. Based on relevant basic theories, scholars have propounded different numerical indexes of rockburst criteria, such as Energy release rate (ERR), Excess shear stress (ESS), Burst potential index (BPI), Local energy release density (LERD), Local energy release rate (LERR), Relative energy release index (RERI), Unit time relative local energy release index (URLERI), etc. (Cook 1965; Bieniawski 1967; Ryder 1988; Wiles 1998; Mitri 1999; Su 2006; Qiu et al. 2014). The above achievements have greatly promoted the development of the rockburst criterion research, but there are few reports on rockburst criterion which is widely used in engineering. However, previous studies on rockburst criteria only considered one or two influencing factors that induce rockburst, which is difficult to accurately determine the rockburst proneness and effectively estimate the rockburst failure degree. As a result, the theoretical research far behind the engineering practice, and there are also deficiencies in engineering applicability. Due to the complexity of rockburst occurrence conditions, the main controlling factors of rockburst are special. Mechanical factors, brittleness factors, energy storage factors, and integrity factors will induce the occurrence of rockburst. How to apply this information to put forward a set of multi-parameter rockburst criterion which can accurately reflect the rockburst formation whole process is an urgent problem to be solved in the basic research related of rockburst.

This paper firstly analyzes the internal relationship between the inoculation mechanism and

the main control factors of rockburst systematically, and selects mechanical factors, brittleness factors, energy storage factors, and integrity factors as the main control factors for the rockburst proneness evaluation. Considering the various stress states of the surrounding rock mass unit, a new criterion evaluation method, the multi-parameter rockburst criterion (RPC) is proposed. Focus on expounding the research ideas and construction methods of RPC, discussing the core theoretical basis and physical significance of the criterion, deeply research on the key factors that have an important control effect on the rockburst failure mechanism, analyzing the control effect and control mechanism of each control factor, puts forward the selection principle of rockburst control factors, and constructs the rockburst intensity classification evaluation system. Secondly, the existing classical rockburst criterion and the newly proposed multi-parameter rockburst criterion are used to verify the accuracy of some typical rockburst engineering examples in China. Finally, based on the 2# diversion tunnel of Jinping II hydropower station, combined with the polycrystalline modeling technology and the three-dimensional discrete element theory, the numerical simulation feasibility of rockburst inoculation and evolution whole process is verified through the three-dimensional discrete element numerical simulation platform, and the accuracy and applicability of the newly proposed multi-parameter rockburst criterion are tested. Then, the numerical simulation analysis of the inoculation mechanism and evolution law of rockburst geological disasters in deep underground engineering under three-dimensional stress condition is carried out, and the dynamic response law of surrounding rock mass under excavation disturbance action in deep underground engineering is studied. The research results are expected to provide basic scientific basis and important theoretical support for the prediction of rockburst.

2 MULTI-PARAMETER ROCKBURST CRITERION FOR DEEP UNDERGROUND ENGINEERING

2.1 Shortcomings of existing rockburst criterions

At present, the rockburst criterion for underground engineering mainly considers the following indicators: maximum principal stress (σ_1), tangential stress (σ_θ), radial stress (σ_r), uniaxial compressive strength of rock (σ_c), tensile strength of rock (σ_t), elastic energy index of rock (W_{et}), integrity coefficient of rock mass (K_v) and lateral pressure coefficient (λ), etc.

Through in-depth analysis of existing rockburst

criteria, it is known that (1) Most rockburst criteria are expressed by radial stress and tangential stress. Coordinate transformation is needed when using numerical simulation software to predict and evaluate rockburst risk in underground engineering excavation process, so the application is quite complicated (Xu et al. 2007; Guo et al. 2015). (2) The evaluation index of rockburst criterion is single, only one or two factors are considered, and the influencing factors of rockburst are not fully considered. (3) According to the definition of rockburst, the surrounding rock stress is one of the necessary conditions to induce rock burst (Wang et al. 1998), and the surrounding rock in the rockburst area is mostly in the three-dimensional stress state, but the existing rockburst criteria are mostly expressed by the maximum principal stress or the maximum tangential stress and the two-dimensional stress state. (4) Most rock burst classifications are more general, and the discriminant indexes used are also different.

2.2 Selection and control mechanism of rockburst control factors

2.2.1 Integrity factor

The engineering practice shows that rockburst mostly occurs in the surrounding rock mass with high energy storage capacity and hard, complete or relatively complete hard and brittle surrounding rock mass. This shows that the rock mass integrity coefficient is an important control factor of rockburst, and the control effect of the rock mass integrity coefficient should be considered in the evaluation process of rockburst proneness. According to literature (Yi et al. 2018), the geological structural conditions also have a significant impact on the integrity of the rock mass, such as regional structures (folds, faults, dikes and lithological conversion zones, etc.) and local structures (faults, joints and closed fissures, structural planes mechanical properties, scale and occurrence). In addition, Reddy and Spotiswoode (2001) investigated the influence of geological structure on the rockburst failure degree through indoor rockburst test. Shang et al. (2013) used tangential stress σ_θ , tensile strength σ_t and integrity index K_v to characterize the rockburst trend and strength. Hu et al. (2020) obtained that the fault structure has a strong control effect on the occurrence of rockburst. The above research results show that the rockburst proneness is related to the integrity of the rock mass.

Based on the previous knowledge and the author's understanding of rock mass integrity factors. Through the rock mass integrity coefficient K_v , the control effect of rock mass integrity on rockburst is semi-quantitatively introduced into the RPC evaluation system, and the control effect of the existence of rock mass geological structure on increasing rockburst proneness, improving failure possibility and increasing failure degree is quantified. Combined with the five-factor rockburst criterion proposed

by Zhang et al. (2008), the rock mass integrity coefficient K_v is shown in Eq. (1).

$$K_v = \begin{cases} < 0.55 & \text{None rockburst} \\ 0.55 \sim 0.60 & \text{Weak rockburst} \\ 0.60 \sim 0.80 & \text{Moderate rockburst} \\ \geq 0.80 & \text{Severe rockburst} \end{cases} \quad (1)$$

2.2.2 Mechanical factor

The surrounding rock mass is in a stress environment that can accumulate high strain energy, which is one of the important conditions for inducing rockburst. The rockburst inoculation process is the mutual synthesis and transformation of a series of mechanical actions, and the connotation of its mechanical behavior is as follows: As shown in Figure 1, before excavation, the deep rock masses are in a true-triaxial equilibrium state ($\sigma_1 > \sigma_2 > \sigma_3$). When one free boundary opens, the stress state of the rock masses near the excavated boundary will be changed, the tangential stress σ_θ increases gradually, the radial stress σ_r decreases rapidly, and the axis stress σ_a varies slightly. After excavation, as a result of the poison effect and surrounding rock deformation effect caused by increasing tangential stress, the radial stress is slightly elevated again and shows a gradient variation. The radial stress on the unloading face is relieved completely. With the increase of the distance away from the unloading face, the radial stress increases. Therefore, the representative rock element near the excavated boundary is in a special stress state, namely, "one face zero load and the other five faces stressed". When the elastic strain energy stored in the surrounding rock mass exceeds the energy lost by the rupture of the rock block, the excess energy will be released in the form of kinetic energy, that is, rock burst occurs. The above analysis shows that the rockburst proneness is related to the mechanical state of the rockburst inoculation process.

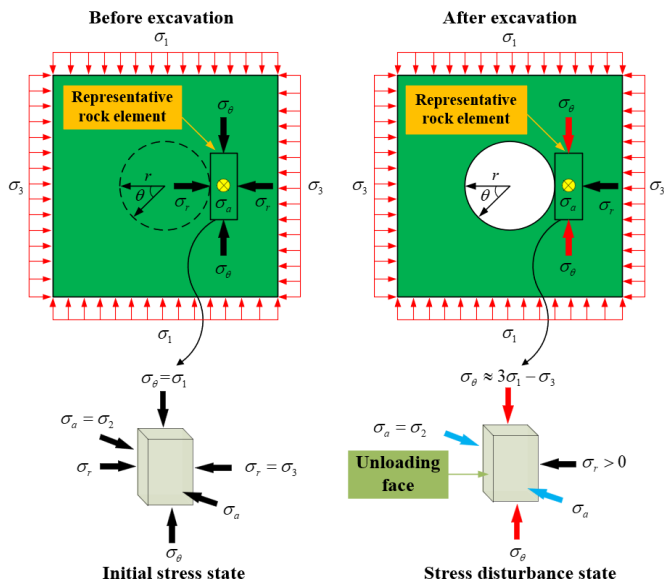


Figure 1. Mechanical environment of rock specimen in underground engineering before and after excavation ($\sigma_1, \sigma_2, \sigma_3$ are initial stresses, and $\sigma_1 > \sigma_2 > \sigma_3$; $\sigma_\theta, \sigma_\alpha, \sigma_r$ are stresses acting on representative rock specimen, and $\sigma_\theta > \sigma_\alpha > \sigma_r$) (adapted from Su et al. 2017)

2.2.3 Brittleness factor

The physical and mechanical properties of the rock can reflect the ability of the rock breaking to generate cracks and the cracks propagation after being stressed, which is usually characterized by the degree of brittleness. The compressive and tensile strengths are the rock strength limit values under the conditions of compressive stress and tensile stress, which can better reflect the characteristics of the overall brittle failure of the rock to a certain extent. The compressive and tensile strengths of rocks can be easily obtained by uniaxial compression and Brazilian splitting tests, so the brittleness evaluation method (Eq.2) based on rock strength characteristics is widely used.

$$B = \frac{\sigma_c}{\sigma_t} \quad (2)$$

Where B is brittleness index; σ_c is the uniaxial compressive strength of rock. σ_t is the tensile strength of rock.

Feng et al. (2000) used uniaxial tensile and compressive strength to calculate the brittleness coefficient of rock, and established the lithology discrimination conditions of rockburst. Altindag (2003) believed that the greater the difference between the compressive strength and the tensile strength of the rock, the higher the brittleness index, and proposed to use the ratio of the two to evaluate the rock brittleness. Wang et al. (1998), Chen et al. (2006), Zhang et al. (2008) believed that the proneness and intensity level of rockburst were closely related to rock brittleness. Figure 2 shows the fitting curves of compressive and tensile strengths with different rocks, in which the data in

the figure are from literature (Ren et al. 2018). It can be seen from Figure 2 that there is a positive correlation between the compressive strength and tensile strength of different rocks, that is, the rocks with higher compressive strength will have higher tensile strength. In view of this, the essence of the problem can be grasped by evaluating the ability of rock to resist high stress damage from the brittleness characteristics of rock.

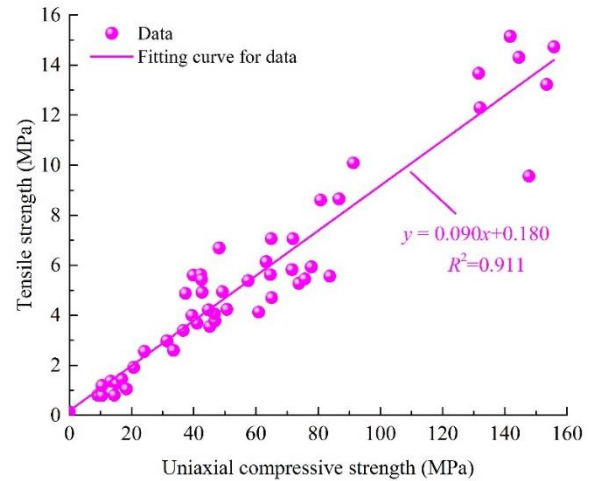


Figure 2. Relationship between compressive strength and tensile strength of rock

2.2.4 Energy storage factor

The accumulation, dissipation and release of energy are the necessary conditions for rockburst. The evaluation of the energy storage and release capacity of the surrounding rock mass is also the assessment of the possibility of dynamic disaster after rock failure. The release level of the energy stored in the surrounding rock mass is very important and indispensable for the evaluation of rockburst proneness. Based on the energy storage characteristics of the surrounding rock mass and the various stress states of the surrounding rock mass unit, the energy factor is reasonably introduced to quantify and evaluate the influence of the energy conversion in the rock deformation process on the rockburst proneness, reflecting the energy evolution and release law of rock in the fracture failure process under different stress states.

(1) Energy conversion mechanism of rock deformation process under stress

The deformation and failure of rock is mainly driven by energy. From the energy point of view, when the rock is deformed under the action of external force, assuming that the physical process has no heat exchange with the outside world, the total input energy generated by the external force is U . According to the principle of energy conservation, the expression of U can be obtained (Xie et al. 2005):

$$U = U_d + U_e \quad (3)$$

Where U_d is the dissipated energy of the rock, which is used to form the internal damage and plastic deformation of the material, as shown in the blank area surrounded by the curve in Figure 3; U_e is the releasable elastic strain energy of the rock, as shown in the shadow area surrounded by the curve in Figure 3.

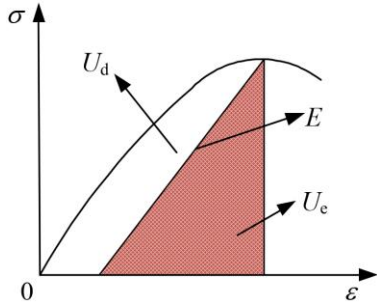


Figure 3. Stress-strain relation curve of rock

The expression of U_e is

$$U_e = \left[\sigma_1^2 + \sigma_2^2 + \sigma_3^2 - 2\nu(\sigma_1\sigma_2 + \sigma_2\sigma_3 + \sigma_1\sigma_3) \right] / 2E \quad (4)$$

Where $\sigma_1, \sigma_2, \sigma_3$ is the three principal stresses corresponding to the maximum value of element strain energy; E is the elastic modulus; ν is the Poisson's ratio.

Based on the energy conversion mechanism of rock deformation process under stress, the difference between dynamic and static failure of rock is explained. The rock is disturbed by the dynamic load to form high stress, which leads to the aggravation of damage of some rock units in a very short period of time and the gradual decrease of strength; the stored elastic strain energy of most rocks rapidly reaches the limit value. U_0 represents the energy required when the rock mass is broken. When $U_e=U_0$, U_e completely releases and rock mass

undergoes static failure; When $U_e > U_0$, the rock mass is damaged dynamically, and the energy difference $\Delta U (\Delta U = U_e - U_0)$ constitutes the kinetic energy of splitting rock mass, which induces rockburst.

(2) Critical energy release rate of rock under different stress paths

The surrounding rock stress is the external cause of the rockburst, and rock itself does not cause the rockburst. Under certain surrounding rock stress conditions, rockburst will occur, and the real power source for rock failure comes from elastic energy release of rock medium caused by stress change. Therefore, the rockburst criterion considering energy factor can more accurately judge the rockburst proneness. To establish RPC, it is necessary to clarify the energy evolution law in the process of rock deformation and failure. In this study, based on the rock strength and overall failure criterion (Xie et al. 2005), the critical energy release rate of rock under different stress paths is obtained.

1) Compression condition ($\sigma_1 > \sigma_2 > \sigma_3 \geq 0$)

A large number of underground engineering practice shows that the surrounding rock stress state before underground cavern excavation is mostly three-dimensional compression (Figure 4(a)). When the rock mass fails as a whole, the elastic strain energy in the principal stress σ_i ($i=1, 2, 3$) direction is proportional to the energy release rate, which is distributed according to the minimum compressive stress difference. Assuming that the energy release rate G_i ($i=1, 2, 3$) is expressed as:

$$G_i = K_i (\sigma_1 - \sigma_i) U_e \quad (5)$$

Where K_i is the material constant.

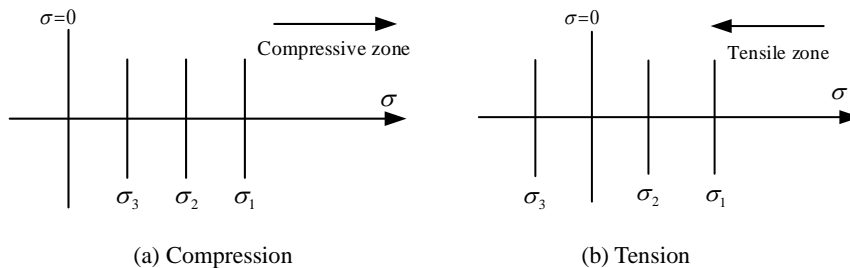


Figure 4. Loading case

It can be seen from Eq. (5) that the maximum energy release rate occurs in the direction of the minimum compressive stress σ_3 , i.e

$$G_3 = K_i (\sigma_1 - \sigma_3) U_e \quad (6)$$

This further shows that the hydrostatic pressure state will not cause the overall failure of rock mass. According to the above analysis, the energy release rate can meet the following requirements when rockburst occurs:

$$G_3 = K_i (\sigma_1 - \sigma_3) U_e \geq G_c \quad (7)$$

Where G_c is the critical strain energy release rate of rockburst under compression state, which is the material constant and can be determined by laboratory rock mechanics test (uniaxial compression test). Let $\sigma_1 = \sigma_c$ and $\sigma_2 = \sigma_3 = 0$, bring them into Eq. (7), it can be obtained by combining Eq. (4):

$$G_c = K_i \frac{\sigma_c^3}{2E} \quad (8)$$

2) Tension condition ($\sigma_3 < 0$)

Tensile stress often occurs in the surrounding rock mass during excavation and unloading of underground engineering, which is also a stress state leading to the overall failure of rock mass. When there is at least one tensile stress in the principal stress (σ_i) of rock element (Figure 4(b)) and the overall failure of rock mass occurs, the elastic strain energy is proportional to the energy release rate in the direction of principal stress, and it is distributed according to the principal stress value. Assuming that the energy release rate G_i ($i=1, 2, 3$) expression is:

$$G_i = K_i \sigma_i U_e \quad (9)$$

By analogy with compression condition, it can be seen from Eq.(9) that the maximum energy release rate G_i occurs in the direction of the maximum tensile stress σ_3 , i.e

$$G_3 = K_i \sigma_3 U_e \quad (10)$$

The energy release rate can meet the following requirements when rockburst occurs:

$$G_3 = K_i \sigma_3 U_e \geq G_t \quad (11)$$

Where G_t is the critical strain energy release rate of rockburst under tension state, which is the material constant and can be determined by laboratory rock mechanics test (uniaxial tensile test). Let $\sigma_3=\sigma_t$ and $\sigma_1=\sigma_2=0$, bring them into Eq. (11), it can be obtained by combining Eq. (4):

$$G_t = K_i \frac{\sigma_t^3}{2E} \quad (12)$$

To sum up, the critical energy release rate of rock under different stress paths is:

$$\text{RPC} = \begin{cases} K_v^2 \cdot \frac{G_3}{G_c} = K_v^2 \cdot \frac{(\sigma_1 - \sigma_3) 2EU_e}{\sigma_c^3} = K_v^2 \cdot \frac{\sigma_1 - \sigma_3}{\sigma_c} \cdot \frac{\sigma_c \sigma_t}{\sigma_t} \cdot \frac{2EU_e}{\sigma_c^3} \\ \qquad \qquad \qquad = K_v^2 \cdot (\sigma_1 - \sigma_3) \sigma_t \cdot \frac{\sigma_c}{\sigma_t} \cdot \frac{2EU_e}{\sigma_c^4} \quad , \quad \sigma_3 \geq 0 \\ K_v^2 \cdot \frac{G_3}{G_t} = K_v^2 \cdot \frac{2EU_e \sigma_3}{\sigma_t^3} = K_v^2 \cdot \frac{\sigma_3}{\sigma_c} \cdot \frac{\sigma_c}{\sigma_t} \cdot \frac{2EU_e}{\sigma_t^2} \quad , \quad \sigma_3 < 0 \end{cases} \quad (14)$$

It can be seen from Eq. (14) that: (1) RPC analysis model reflects the integrity factor (K_v), mechanical factor $(\sigma_1 - \sigma_3)\sigma_t$ or σ_3/σ_c , brittleness factor (σ_c/σ_t) and energy storage factor $(U_e/\sigma_c^4$ or $U_e/\sigma_c^2)$ of rockburst incubation process. (2) RPC is the product of main stress in mathematical expression, which is easy to understand, use and operate. (3) RPC not only considers the stress state ($\sigma_1, \sigma_2, \sigma_3$) of surrounding rock and the integrity of rock mass, but also reflects the influence of rock

$$\begin{cases} G_c = K_i \frac{\sigma_c^3}{2E} \quad , \quad \sigma_3 \geq 0 \\ G_t = K_i \frac{\sigma_t^3}{2E} \quad , \quad \sigma_3 < 0 \end{cases} \quad (13)$$

2.3 Determining the threshold and intensity classification of multi-parameter rockburst criterion

(1) Determining RPC Mathematical Forms

There are various mathematical forms of past empirical indicators, such as the product quotient form of the rock mass quality Q-system, the sum-adding form of the surrounding rock mass classification RMR system, and the product quotient or sum-adding form with weight coefficients (Qiu et al. 2011). No matter which form is adopted, one principle is followed in the construction process of RPC, that is, the principle of monotonically increasing RPC value. This shows that the control factors considered should be factors that play a positive role in the evaluation process of rockburst proneness, and there should be no coupling phenomenon between the control factors. In order to clearly distinguish the RPC values corresponding to different levels of rockburst proneness and take into account the logical relationship of "and" between the main control factors and discriminant indexes. In this paper, the product form similar to the Q system was selected to construct the RPC mathematical form, as shown in Eq. (14). The biggest difference between the RPC form and the Q-system method is that the side effect factor on rockburst proneness is not introduced.

mechanical parameters (σ_c, σ_t) and deformation parameters (E, ν).

(2) Determining RPC threshold and intensity classification

The above sections have clarified the selection method and the corresponding determination method of rockburst control factors in RPC. In order to apply RPC to judge rockburst proneness and failure degree, it is also necessary to study the relationship between RPC thresholds and rockburst intensity.

Based on the division of elastic energy index limit value and rockburst potential limit value proposed by Zhang et al. (2008) and Shang et al. (2013) and taking the measured rockburst data of Tiantaishan tunnel (Table 1) as the simulation sample, the results are shown in Table 2. Among them, K_u is the deformation brittleness coefficient, σ_{max} is the maximum principal stress of the surrounding rock mass, σ_c/σ_{max} is the strength ratio of the surrounding rock mass. Considering that the probability of the boundary index of different factors reaching the

maximum value at the same time is small, in order to facilitate practical application, the boundary indexes of RPC are set to 2, 11 and 110. Therefore, the rockburst criterion and its intensity classification are as follows:

$$RPC = \begin{cases} < 2 & \text{None rockburst} \\ 2 \sim 11 & \text{Weak rockburst} \\ 11 \sim 110 & \text{Moderate rockburst} \\ > 110 & \text{Severe rockburst} \end{cases} \quad (15)$$

Table 1. Measured data for rockburst at Tiantaishan tunnel

No.	Position/m	σ_i/MPa			Poisson ratio	K_v	σ_c/MPa	σ_t/MPa
		σ_1	σ_2	σ_3				
TSE5	108	16.15	8.14	4.27	0.28	0.68	130.21	11.55
	150	19.23	10.51	3.16			141.13	13.68
	271~350	20.22	12.53	3.58			169.52	15.14
	500~550	40.57	24.12	12.36			192.15	18.86
TSE6	350	23.65	10.87	4.02			175.65	17.26
	500	35.86	21.44	15.61			184.27	18.34

Table 2 Simulated results for rockburst at Tiantaishan tunnel (Zhang et al. 2008; Guo et al. 2015)

No.	Position/m	Rockburst intensity	Evaluation results of different evaluation methods					
			K_u	Rockburst intensity	σ_c/σ_{max}	Rockburst intensity	RPC	Rockburst intensity
TSE5	108	Weak	3.1	Weak	8.1	Weak	0.8	None
	150	Moderate	2.7	Weak	7.3	Weak	2.7	Weak
	271~350	Weak	2.7	Weak	8.4	Weak	1.5	None
	500~550	Moderate	2.8	Weak	4.7	Weak	7.6	Weak
TSE6	350	Weak	-	-	7.4	Weak	1.4	None
	500	Moderate	-	-	5.1	Moderate	11.6	Moderate

2.4 Application and verification of multi-parameter rockburst criterion

In order to further verify the accuracy, rationality, validity and reliability of RPC, taking rockburst disaster of typical engineering as examples (Table 3), Hoek criterion, Russenes criterion, Erlangshan highway tunnel criterion, Gu-Tao criterion and the RPC proposed in this paper were tested respectively. The results were compared with the actual rockburst intensity grade, as shown in Table 4 and Figure 5. Among them, the values of σ_2 and σ_3 refer to the distribution law of in-situ stress in China (Cai et al. 2013) and are supplemented by combining in-situ stress test results.

(1) Hoek criterion

$$\sigma_{max}/\sigma_c = \begin{cases} 0.34 & \text{None rockburst} \\ 0.42 & \text{Weak rockburst} \\ 0.56 & \text{Moderate rockburst} \\ > 0.70 & \text{Severe rockburst} \end{cases} \quad (16)$$

(2) Russenes criterion

$$\begin{cases} \sigma_\theta/\sigma_c < 0.2 & \text{None rockburst} \\ \sigma_\theta/\sigma_c = 0.2-0.3 & \text{Weak rockburst} \\ \sigma_\theta/\sigma_c = 0.3-0.55 & \text{Moderate rockburst} \\ \sigma_\theta/\sigma_c > 0.55 & \text{Severe rockburst} \end{cases} \quad (17)$$

(3) Erlangshan highway tunnel criterion

$$\begin{cases} \sigma_\theta/\sigma_c < 0.3 & \text{None rockburst} \\ \sigma_\theta/\sigma_c = 0.3-0.5 & \text{Weak rockburst} \\ \sigma_\theta/\sigma_c = 0.5-0.7 & \text{Moderate rockburst} \\ \sigma_\theta/\sigma_c > 0.7 & \text{Severe rockburst} \end{cases} \quad (18)$$

(4) Gu-Tao criterion

$$\begin{cases} \sigma_c/\sigma_1 > 14.5 & \text{None rockburst} \\ \sigma_c/\sigma_1 = 5.5-14.5 & \text{Weak rockburst} \\ \sigma_c/\sigma_1 = 2.5-5.5 & \text{Moderate rockburst} \\ \sigma_c/\sigma_1 < 2.5 & \text{Severe rockburst} \end{cases} \quad (19)$$

It can be seen from Table 4 and Figure 5: (1) The total number of moderate and severe rockbursts determined by Hoek criterion, Russenes criterion and Erlangshan highway tunnel criterion is relatively close, and the number of weak rockburst determined by Hoek criterion is slightly higher than that determined by Russenes criterion and Erlangshan highway tunnel criterion. (2) The rockburst grade determined by the Gu-Tao criterion is mainly concentrated in the moderate rockburst, and the total number of weak and severe rockbursts is relatively close, which indicates that the determination accuracy of Gu-Tao criterion is slightly lower than that of Hoek criterion, Russenes criterion and Erlangshan highway tunnel criterion. (3) The total number of weak and moderate rockbursts determined by the rockburst proneness criterion in this paper is close to the actual situation,

but its performance in the determination of severe rockburst grade is weak. By comprehensive comparison, the accuracy of the criterion presented in this paper is obviously higher than that of the other four criteria, and it is basically consistent with the actual occurrence of rockburst on the whole, which has good engineering applicability.

In summary, the multi-parameter rockburst criterion established in this study is of clear significance, simple and practical, which can reasonably and quantitatively determine the occurrence and intensity grade of rockburst geological disasters in the process of deep underground engineering construction. This criterion comprehensively considers various stress states of surrounding rock mass unit. It comprehensively considers the integrity factors, mechanical factors, brittle factors and energy storage factors in the process of rockburst inoculation. This criterion is more targeted for rockburst prediction and evaluation, and it has good engineering applicability. It is of great significance to use numerical calculation software to simulate and predict rockburst disasters in deep underground engineering.

Table 3. Initial data for rockburst analysis in some projects (Shang et al. 2013; Guo et al. 2015)

No.	Project name	Buried depth/m	Principal stress/MPa			τ_{max}/MPa	σ_c/MPa	K_v
			σ_1	σ_2	σ_3			
1	Jinping I	400	9.00	8.44	4.50	18~70	50~70	0.34~0.72
			35.00	17.50	10.80			
2	Jinping II	1200~2500	38.00	32.40	19.00	55~108	110~120	0.76
			71.00	67.50	35.50			
3	Headrace tunnel for TianshengqiaoII hydropower station	130~760	25.80	12.90	3.51	30	88.7	0.75
			25.80	20.52	12.90			
4	Headrace tunnel for Taipingyi hydropower station	400	31.40	15.70	10.80	62.6	130~180	0.75
5	Qinling Railway Tunnel	1600	20.00	18.75	10.00	105	95~130	0.75
			40.00	37.50	20.00			
6	Linglong Gold Mine, Shandong Province	1000	50.00	27.00	25.00	82~114	138~197	0.75
			60.00	30.00	27.00			
7	Erlang Mountain road	770	53.70	26.85	20.79	41.46	64.9	0.75
8	Dongguashan Copper Mine, Tongling	790~850	34.33	21.33	17.17	105.5	132.2	0.75
			34.33	22.95	17.17			
			57.20	28.60	10.80			
9	Underground caverns of Pubugou hydropower station	250~320	27.30	13.65	8.64	42~54	82.3~207.5	0.80
			21.10	10.55	6.75			
10	Diversion tunnel for Yuzixi class I hydropower station	250~600	45.00	22.50	16.20	90	170	0.80
			30.00	15.00	6.75			
11	Tai-Jin Expressway Cangling Tunnel	300~756	59.50	29.75	8.10	48.9	150	0.75
			59.50	29.75	20.41			

Table 4. Verification of rockburst in rock engineering projects (Guo et al. 2015)

No.	σ_i /MPa	Hoek criterion		Russenes criterion	Erlang Mountain tunnel criterion	Gu-Tao criterion		RPC	
		Threshold	Rockburst intensity	Rockburst intensity	Rockburst intensity	Threshold	Rockburst intensity	Thres hold	Rockburst intensity
1	5.0	0.36	Weak	Moderate	Weak	5.56	Weak	0.4	None
		1.40	Severe	Severe	Severe	1.43	Severe	10.6	Weak
2	5.0~6.0	0.50	Moderate	Moderate	Moderate	2.89	Moderate	137.9	Severe
		0.46	Weak	Moderate	Weak	1.55	Severe	569.9	Severe
3	3.7	0.34	Weak	Weak	Weak	3.44	Severe	23.8	Moderate
		0.34	Weak	Weak	Weak	3.44	Severe	98.8	Moderate
4	9.4	0.35~0.48	Weak-Moderate	Weak-Moderate	Weak	4.14~5.73	Moderate-Intense	6.2	Weak
5	7.0	1.11	Severe	Severe	Severe	4.75~6.50	Weak-Moderate	7.7	Weak
		0.81	Severe	Severe	Severe	2.38~3.25	Moderate	61.7	Moderate
6	7.0~10.0	0.59	Moderate	Severe	Moderate	2.76	Moderate	90.9	Moderate
		0.42	Weak	Moderate	Weak	3.94	Moderate	31.2	Moderate
7	8.0	0.64	Moderate	Severe	Moderate	1.21	Severe	56.6	Moderate
		0.80	Severe	Severe	Severe	3.85	Moderate	2.4	Weak
8	16.4	0.80	Severe	Severe	Severe	3.85	Moderate	2.4	Weak
		0.80	Severe	Severe	Severe	3.85	Moderate	2.4	Weak
9	5.9	0.20~0.51	Weak-Moderate	Weak-Moderate	Weak-Moderate	3.01~7.60	Weak-Moderate	17.3	Moderate
		0.26~0.66	Weak-Moderate	Weak-Moderate	Weak-Moderate	3.90~9.83	Weak-Moderate	8.1	Weak
10	11.3	0.53	Moderate	Moderate	Moderate	3.78	Moderate	12.5	Moderate
		0.53	Moderate	Moderate	Moderate	5.67	Weak	2.4	Weak
11	8.0	0.33	Weak	Weak	Moderate	2.52	Moderate	28.9	Moderate
		0.33	Weak	Weak	Moderate	2.52	Moderate	68.3	Moderate

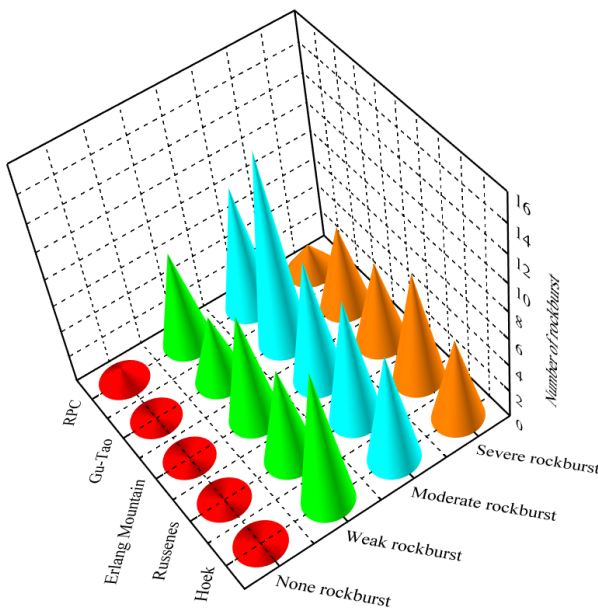


Figure 5 Comparison of rockburst results with different criteria

In this section, through the secondary development of the three-dimensional discrete element numerical simulation software, the three-dimensional discrete element theory and polycrystalline modeling technology are coupled to construct a three-dimensional Voronoi polycrystalline discrete element model. Firstly, the three-dimensional discrete element simulation of the rockburst ejection whole process of hard rock specimen under true triaxial single face unloading is carried out, and the numerical simulation feasibility of the whole process of rockburst inoculation and evolution is verified by comparing the test results. Finally, the numerical simulation research on the inoculation mechanism and evolution law of rockburst geological disasters in deep underground engineering under three-dimensional stress conditions is carried out, and the accuracy and applicability of the newly proposed multi-parameter rockburst criterion are tested.

3.1 Simulation of hard rockburst ejection whole process under single face unloading condition

The comparison of rock specimens rockburst

3 THREE-DIMENSIONAL DISCRETE ELEMENT REALIZATION OF MULTI-PARAMETER ROCKBURST CRITERION

ejection failure process between test and simulation is shown in Figure 6. The experimental figures are cited from Su et al (2016). The numerical results reproduce macroscopically and phenomenologically the overall fracturing process of rockbursts including the nucleation, propagation, coalescence, interaction, and through-going of cracks.

It can be seen from Figure 6 that small grains ejection firstly appeared on the unloading face of the rock sample, and then the rock plate spalled and swelled outwards. At the same time, fragments were peeled off and the size was getting larger and larger, making the failure zone in the upper part of the rock sample expand from point to surface. Finally, the

rock plate broke and the fragments were ejected immediately. The failure process of rockburst ejection can be summarized as four stages: grains ejection, rock spalling into plates, rock shearing into fragments, and rock fragments ejection. These four stages occurred sequentially within a short period. The uneven force on the unloading face causes local cracking or small grains ejection, and then the surface unit of the unloading face spalling rock into the plate, and the rock sample behind the rock plate was shearing into blocks to form potential rockburst pits, and then the rock plate was continuously bent, Once the rock plate is broken, the rockburst occurred immediately.

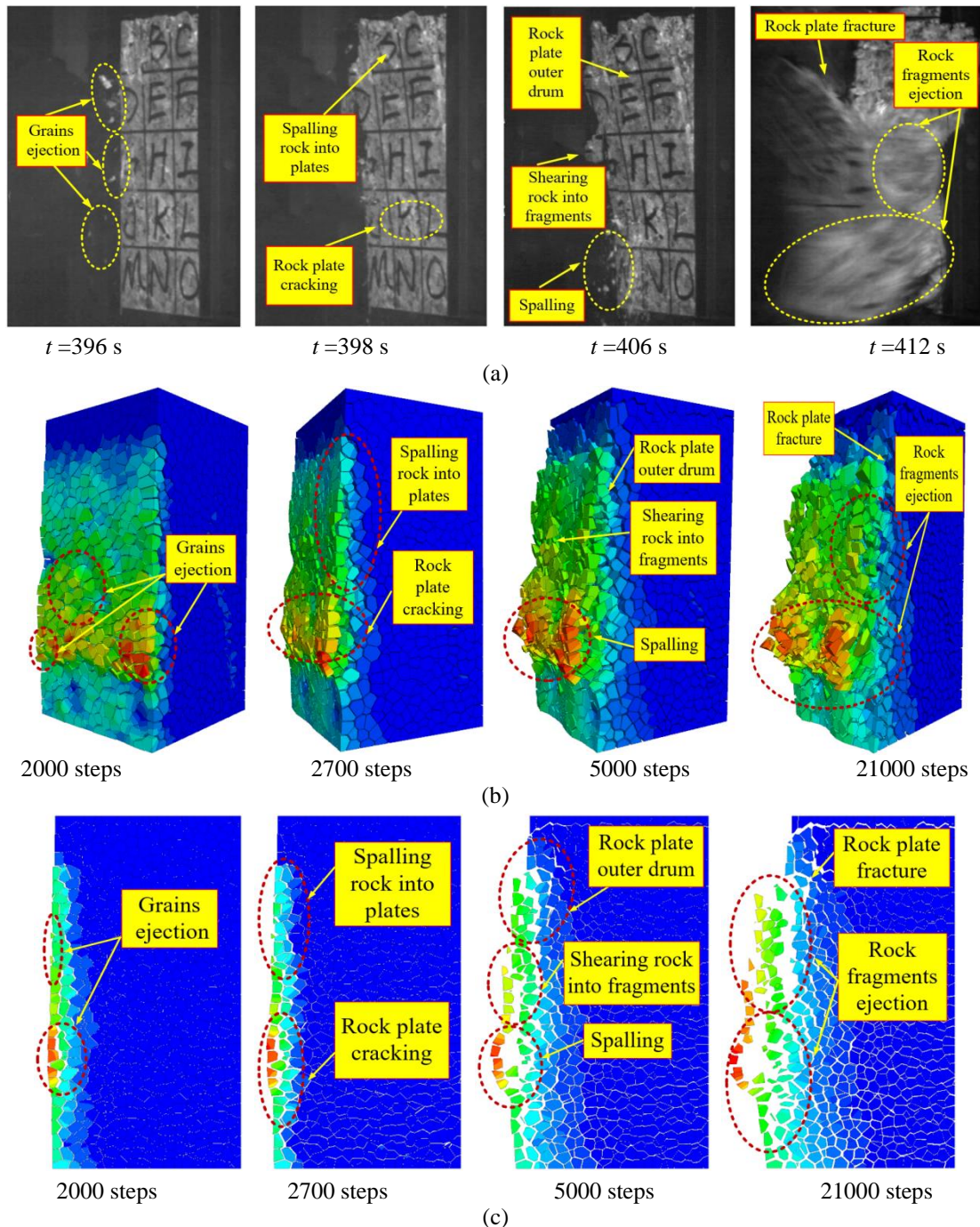


Figure 6. Comparison of rock specimens rockburst ejection failure process between test and simulation. a Physical testing results; b Numerical simulation results (Three-Dimensional); c Numerical simulation results (Central section)

From the above analysis, the numerical simulation results are relatively close to the experimental results, verifying the correctness and rationality of the numerical simulation. It can be known that the three-dimensional Voronoi polycrystalline discrete element model can better reflect the initiation, expansion, convergence and penetration of microcracks and the entire process of macroscopic crack formation. It can also intuitively describe the spalling of rock elements, the rockburst precursors of the continuous bending of plates and rock plates, and the whole process of rockburst inoculation and evolution of the rock masses ejected outward after the plate is broken. Reproducing the ejection failure process of rockburst from continuous failure to discontinuous large deformation failure is beneficial to understanding the mechanism of the rockburst ejection from the micro to the macro level. This shows that the discrete element method has great potential in studying the discontinuous deformation and failure process of rocks.

3.2 Simulation of rockburst disaster in deep underground engineering

3.2.1 Calculation model and boundary conditions

The 2# diversion tunnel of Jinping II hydropower station was excavated from east to west. When the excavation reached the K11+027~K11+046 section, a severe rockburst occurred from the north wall to the spandrel (Figure 7) (Zhou et al. 2015). The depth of rockburst pit is about 2 m. Through field investigation, it is not found that there is a control structural plane in this section, and the surrounding rock is fresh and complete, which is mainly T_{2b} marble. The section

size of 2# diversion tunnel is shown in Figure 8. According to the field monitoring results (Zhou et al. 2015), the ground stress level of the tunnel section was high, which was shown in Table 5.



Figure 7. Rockburst location of 2# diversion tunnel

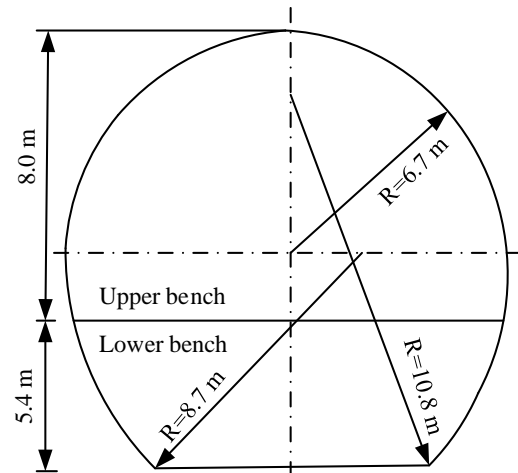


Figure 8. Dimension of 2# diversion tunnel

Table 5. In-situ stress state of 2# diversion tunnel

Buried depth/m	σ_x /MPa	σ_y /MPa	σ_z /MPa	τ_{xy} /MPa	τ_{yz} /MPa	τ_{zx} /MPa
1900	48.54	49.97	51.46	0.35	3.23	5.82

According to the Saint-Venant principle and the influence range of tunnel excavation, the calculation model was established with 90 m transverse length, 80 m vertical height and 50 m longitudinal width. The numerical model is shown in Figure 9 and the arrangement of monitoring points is shown in Figure 10. In the dynamic calculation, in order to make the dynamic energy of the system absorb quickly and achieve convergence, Rayleigh damping was used, the minimum critical damping ratio was 0.05, and the minimum center frequency was 500 Hz. The upper boundary of the calculation model was the stress constraint boundary condition, and the vertical load of 51.46 MPa (field measurement) was applied.

The lower boundary, front and rear boundary and left and right boundary of the calculation model were all displacement constraint boundary conditions. The peripheral boundary of the model was set as a static boundary, and dampers were set in the normal and tangential directions of the model to reduce or eliminate the elastic wave reflection generated by the simulation calculation, which provided the constraint effect equivalent to the infinite site for the calculation model.

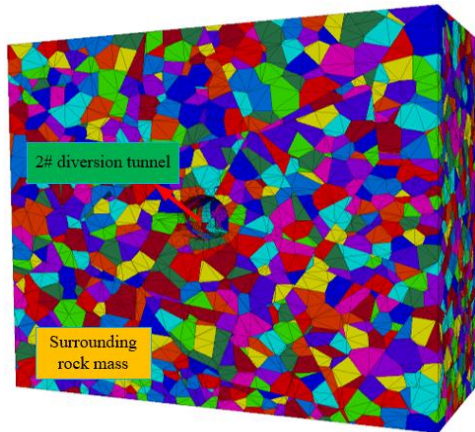


Figure 9. Numerical model

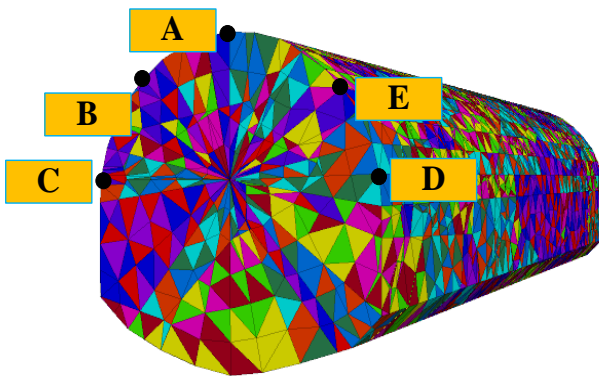


Figure 10. Monitoring point position of 2# diversion tunnel

3.2.2 Action form of blasting load

Since rockburst is a complex process generated instantaneously, detonating the pre-buried explosive in the cavern will instantly generate irresistible high temperature and high-pressure gas, which expand rapidly in the interior of the cavern. The blast shock wave generated acts on the inner wall of the cavern and rapidly attenuates to stress wave. The whole process is very short, and the duration is only a few milliseconds. Because the explosion mechanism and its influencing factors are extremely complex, it is difficult to quantitatively determine the details of the explosion process. In the numerical analysis, the blasting load is often assumed to be a triangular shock wave (Zhou et al. 2020), and the expression of the blasting load history curve of the triangular function is shown in Eq. (20). Through the secondary development of three-dimensional discrete element software, the dynamic load is

applied by using FISH programming language, which is applied to the tunnel excavation profile by using APPLE command.

$$p(t) = \begin{cases} 0 & t < 0, t > t_d \\ \frac{t}{t_r} p_m & 0 \leq t \leq t_r \\ \frac{t_d - t}{t_d - t_r} p_m & t_r \leq t \leq t_d \end{cases} \quad (20)$$

Where $p(t)$ is the blasting load pressure value at any moment; p_m is the peak blasting load, $p_m=60$ MPa; t_r is the time when the blasting load rises to the peak, $t_r=0.3$ ms; t_d is the time for the positive pressure of the blasting load, $t_d=1$ ms.

3.2.3 Constitutive relation and yield criterion

In the numerical simulation, the selection of the constitutive model needs to have a high degree of conformity with the mechanical properties of engineering materials. The Mohr-Coulomb yield criterion, which describes the mechanical behavior of hard rock, is adopted for the constitutive relation of the model to truly reflect the stress condition of surrounding rock (Shi et al. 2016). The failure envelope of the criterion corresponds to the shear yield function and the tensile stress yield function, which is a flow rule related to the tensile failure.

The physical and mechanical parameters of surrounding rock refer to the inversion results of ground stress and mechanical parameters of rock mass of Jinping Project Group, Institute of Rock and Soil Mechanics, Chinese Academy of Sciences, as shown in Table 6, where E is the elastic modulus, ν is poisson's ratio, c_m is the peak value of cohesion, c_r is the residual value of cohesion, φ_0 is the initial value of friction angle, φ_m is the peak value of friction angle, and ψ is the dilatancy angle. The rock lithology is assumed in the numerical calculation: the rock is homogeneous, isotropic continuum, which conforms to Mohr-Coulomb strength criterion, and the material parameters meet Mohr-Coulomb constitutive model.

Table 6. Physical and mechanical parameters of rock

E/GPa	ν	c_m/MPa	c_r/MPa	$\varphi_0/^\circ$	$\varphi_m/^\circ$	$\psi/^\circ$
18.9	0.23	15.6	7.4	25.8	39.0	10.0

3.2.4 Analysis of numerical simulation results

The middle position of the rockburst area (near K11+037) was selected for analysis. In the numerical simulation, the FISH programming language embedded in three-dimensional discrete element software was used to write calculation functions for Eq. (4) and Eq.(14), and the change process of all calculation block units was monitored. In this section, the rockburst proneness would be evaluated according to the numerical simulation results and the prediction evaluation indexes.

(1) Analysis of energy release evolution process

According to the numerical simulation results, the distribution state of elastic strain energy density was shown in Figure 11, the contour nephogram of principal stress difference was shown in Figure 12, and the space-time distribution of elastic strain energy density was shown in Figure 13. From the above figure, it could be seen that the maximum principal stress difference was mostly concentrated in the right spandrel, side wall and arch bottom of the cavern after excavation. According to the rock mechanics theory, the energy storage limit of rock mass at the maximum principal stress difference will increase significantly. Combined with the cloud map of the elastic strain energy density distribution, it was found that the surrounding rock masses close to the empty surface of the cavern under the disturbance of dynamic excavation had different degrees of elastic strain energy release phenomenon, and the amount of elastic strain energy release gradually decreased with the increase of the distance to the center of the tunnel. The elastic strain energy release of surrounding rock at the right spandrel, side wall and arch bottom of the cavern was the largest, which further indicated that the gentle acceleration process of rock fracture evolution around the cavern is also the process of energy accumulation and dissipation in the surrounding rock. The stress of surrounding rock was highly concentrated, which increased the energy accumulation. When the storage energy of surrounding rock exceeded the energy storage limit of rock mass, the excess energy was released rapidly in the form of kinetic energy, resulting in rockburst.

The rockburst simulation was shown in Figure 14. It could be seen from Figure 14 that the largest rockburst pit of the tunnel was located at the right side wall and spandrel of the tunnel face, which was close to the field situation, and the depth of the largest rockburst pit was about 2 m, as shown in

Figure 15. According to the failure shape of the tunnel, the numerical simulation results were basically consistent with the shape of the actual rockburst pit (Figure 16), which verified the rationality of the prediction and evaluation of the rockburst criterion in this paper and could meet the requirements of dynamic tracking of the rockburst process.

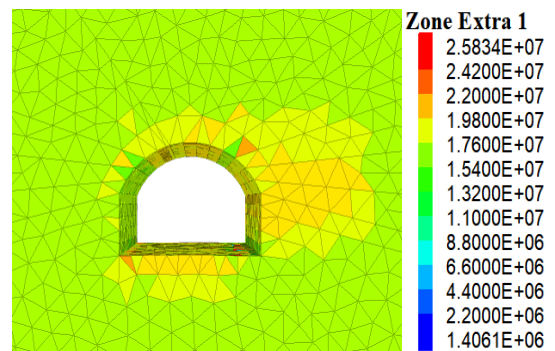


Figure 11. Distribution of elastic strain energy density (unit: J/m^3)

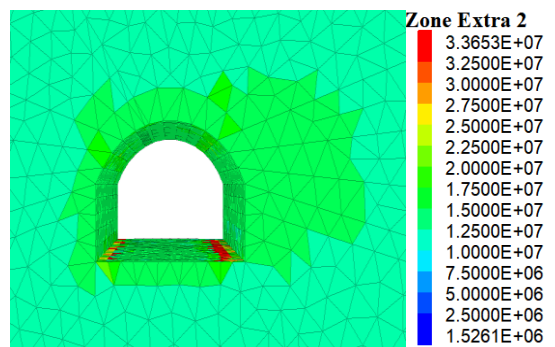


Figure 12. Contour maps of principal stresses difference (unit: Pa)

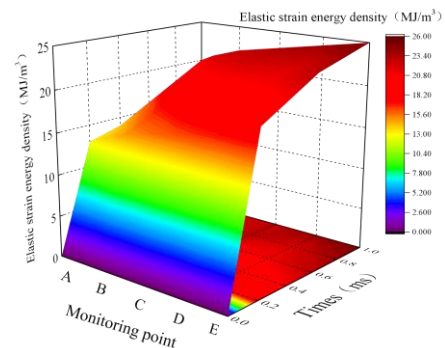


Figure 13. Space-time distribution of strain energy density

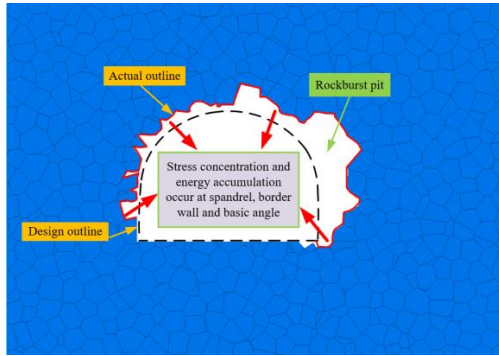


Figure 14. Sketch of rockburst simulation

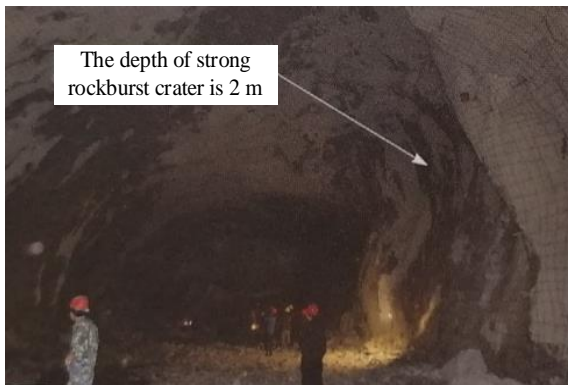


Figure 15. Sketch of rockburst areas in situ (Zhou et al. 2015)

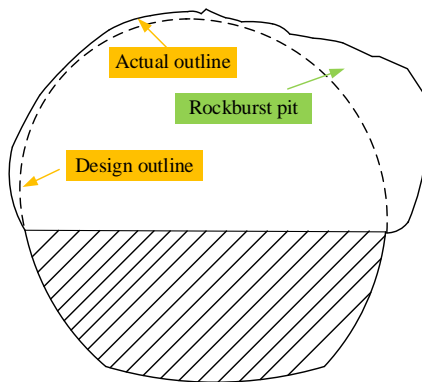


Figure 16. Section outline

(2) Distribution characteristics of RPC

The nephogram of the boundary value distribution of rockburst proneness criterion was shown in Figure 17. From Figure 17, it could be seen that the rockburst criterion RPC boundary value at different locations of the tunnel section showed a completely different change rule. Details were as follows: at the right spandrel position of the cavern, the RPC boundary value reached the maximum 121.23; at the junction of the spandrel and the side wall on both sides of the cave, the RPC boundary values were mostly concentrated between 40 and 85, which could release some elastic strain energy and had the possibility of moderate rockburst; at the left spandrel of the cavern, the RPC boundary values were mostly concentrated between 95 and 120, and there was a possibility of severe rockburst. This shows that the surrounding rock accumulates a

large number of elastic strain energy under the influence of high stress. When the surrounding rock strength exceeds the ultimate strength of the rock mass, the surrounding rock occurs brittle failure and instantaneous releases a large number of elastic strain energy, and then the rockburst phenomenon of rock block spalling, ejection and even throwing occurs.

Taking the arch foot on the right side of the cavern as the center of the circle and rotating counterclockwise for one round, the RPC boundary value of the cavern cross section ($0^{\circ}\sim 360^{\circ}$) of the section K11+037 was obtained, as shown in Figure 18. According to the analysis of Figure 18, the maximum value of RPC boundary value appeared on the surrounding rock surface of the cavern spandrel (about $70^{\circ}\sim 85^{\circ}$). When the angle was $0^{\circ}\sim 90^{\circ}$, the boundary value of RPC was 12~96, and there was a possibility of weak to severe rockburst. When the angle was $90^{\circ}\sim 180^{\circ}$, the boundary value of RPC was 30~95, and there was a possibility of moderate to severe rockburst. When the angle was $180^{\circ}\sim 240^{\circ}$, the boundary value of RPC was 25~70, and there was a possibility of moderate rockburst. When the angle was $240^{\circ}\sim 360^{\circ}$, the boundary value of RPC was 45~90, and there was a possibility of moderate to severe rockburst. From the above analysis, it could be seen that the RPC boundary value obtained by numerical simulation was consistent with the case of severe rockburst in practical engineering.

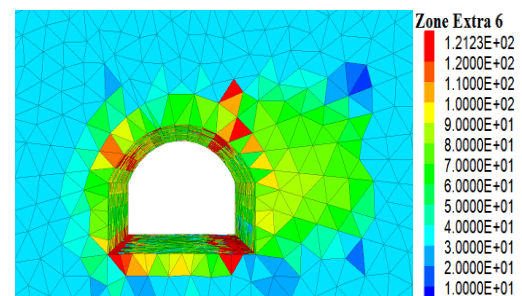


Figure 17. Contour maps of RPC thresholds

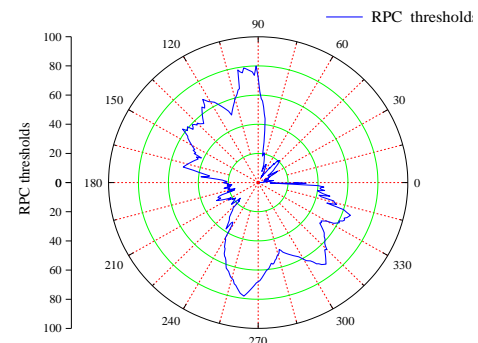


Figure 18. Rockburst criterion thresholds of K11+037 section ($0^{\circ}\sim 360^{\circ}$)

4 CONCLUSIONS

Based on the energy principle, this paper takes mechanical factor, brittleness factor, energy storage factor and integrity factor as the main control factors of rockburst proneness evaluation, comprehensively considers various stress states of surrounding rock mass unit and establishes a new multi-parameter rockburst criterion (RPC). Combined with polycrystalline modeling technology and three-dimensional discrete element theory, some typical rockburst engineering examples are verified, and the simulation study of the whole process of tunnel rockburst inoculation and evolution is realized. The conclusions are as follows:

(1) The research ideas and construction methods of the multi-parameter rockburst criterion are expounded, the core theoretical basis and physical significance of the criterion are discussed, the energy source of rockburst disaster and the transfer form in the occurrence process are clarified, the control function and control mechanism of each control factor are analyzed. Four key control factors in the rockburst proneness evaluation process were determined: mechanical factors, brittleness factors, energy storage factors, integrity factors, built a bridge between rockburst failure degree and rockburst control factors, and a new rockburst criterion and rockburst classification evaluation system was established.

(2) The mathematical expression of multi-parameter rockburst criterion is simple, the physical meaning is clear, and it is simple and practical. Only the surrounding rock mass stress, the tensile strength and compressive strength of rock, the elastic modulus and Poisson's ratio and the integrity coefficient of rock mass are measured, which avoids the calculation of tangential stress and radial stress of complex surrounding rock mass. More importantly, the criterion comprehensively considers various stress states of the surrounding rock mass unit, and the mathematical expression is expressed in the principal stress product form. No coordinate transformation is required when using numerical simulation software to simulate, which is easy to use and operate.

(3) The accuracy and applicability of some typical rockburst engineering examples in China are verified by using Hoek criterion, Russenes criterion, Erlangshan highway tunnel criterion, Gu-Tao criterion and RPC newly proposed in this paper, and the results are compared with the on-site rockburst intensity. It is concluded that the correct judgments number and the correct rate of RPC are significantly higher than the other four criteria, which indicates that RPC has certain applicability in the evaluating the rockburst failure degree and rockburst intensity

and provides a new way to solve the problem of rockburst proneness evaluation in deep buried tunnel.

(4) The numerical calculation and analysis of typical rockburst engineering examples show that the prediction and evaluation of rockburst by multi-parameter rockburst criteria is basically consistent with the actual situation of rockburst, which can reflect the overall trend of rockburst failure in deep-buried tunnels. It has good reliability and can be widely used in rock engineering with rockburst proneness. The basic idea of constructing the criterion and the evaluation method of rockburst failure degree and rockburst proneness based on this criterion can be extended to similar underground engineering, which has good effectiveness and engineering applicability, and can provide reference for rockburst prediction of similar deep engineering.

ACKNOWLEDGEMENTS

This work is financially supported by the National Natural Science Foundation of China (Grant No.: 51474097).

All the authors declare that there is no conflict of interest regarding the publication of this paper.

REFERENCES

- Altindag R., Correlation of specific energy with rock brittleness concepts on rock cutting, *Journal of the South African Institute of Mining and Metallurgy*, Vol. 103, No. 3, 2000, pp 163-171.
- Barton N., Lien R., Lunde J., Engineering classification of rock masses for the design of tunnel support, *Rock Mechanics*, Vol. 6, No. 4, 1974, pp 189-236.
- Bieniawski Z. T., Mechanism of brittle fracture of rock, *International Journal of Rock Mechanics and Mining Sciences & Geomechanics Abstracts*, Vol. 4, No. 4, 1967, pp 405-430.
- Cai M. F., He M. C., Liu D. Y., 2013. *Rock mechanics and Engineering*. Beijing: Science Press.
- Chen B. R., Feng X. T., Xiao Y. X., Ming H. J., Zhang C. S., Hou J., Chu W. J., Acoustic Emission Test on Damage Evolution of Surrounding Rock in Deepburied Tunnel during TBM Excavation, *Chinese Journal of Rock Mechanics and Engineering*, Vol. 29, No. 8, 2010, pp 1562-1569.
- Chen L. W., Bai S. F., Proportioning test study on similar material of rockburst tendency of brittle rockmass, *Rock and Soil Mechanics*, Vol. 27, No. S2, 2006, pp 1050-1054.
- Cook N. G., A note on rockbursts considered as a problem of stability, *South African Institute of Mining and Metallurgy*, Vol. 5, No. 65, 1965, pp 437-446.
- Feng T., Xie X. B., Wang W. X., Pan C. L., Brittleness of Rocks and Brittleness Indexes for Describing Rockburst Proneness, *Mining and Metallurgical Engineering*, Vol. 20,

- No. 4, 2000, pp 18-19.
- Feng X. T., Xiao Y. X., Feng G. L., Yao Z. B., Chen B. R., Yang C. X., Su G. S., Study on the development process of rockbursts, *Chinese Journal of Rock Mechanics and Engineering*, Vol. 38, No. 4, 2019, pp 649-673.
- Feng X. T., Zhang C. Q., Chen B. R., Feng G. L., Zhao Z. N., Ming H. J., Xiao Y. X., Duan S. Q., Zhou H., Dynamical control of rockburst evolution process, *Chinese Journal of Rock Mechanics and Engineering*, Vol. 31, No. 10, 2012, pp 1983-1997.
- Gong F. Q., Wang Y. L., Luo S., Rockburst proneness criteria for rock materials: Review and new insights, *Journal of Central South University*, Vol. 27, No. 10, 2020, pp 2793-2821.
- Gu M. C., He F. L., Chen C. Z., Study on rockburst in Qinling tunnel, *Chinese Journal of Rock Mechanics and Engineering*, Vol. 21, No. 9, 2002, pp 1324-1329.
- Guo J. Q., Zhao Q., Wang J. B., Zhang J., Rockburst prediction based on elastic strain energy, *Chinese Journal of Rock Mechanics and Engineering*, Vol. 34, No. 9, 2015, pp 1886-1893.
- Hoek E. P., Brown E. T., Practical estimates of rock mass strength, *International Journal of Rock Mechanics and Mining Sciences*, Vol. 34, No. 8, 1997, pp 1165-1186.
- Hu L., Feng X. T., Xiao Y. X., Wang R., Feng G. L., Yao Z. B., Niu W. J., Zhang W., Effects of structural planes on rockburst position with respect to tunnel cross-sections: a case study involving a railway tunnel in China, *Bulletin of Engineering Geology and the Environment*, Vol. 79, 2020, pp 1061-1081.
- John C. J., Neville G. W., Fundamentals of rock mechanics, *Science Paperbacks*, Vol. 9, No. 3, 1979, pp 251-252.
- Karchevsky A. L., Determination of the possibility of rock burst in a coal seam, *Journal of Applied and Industrial Mathematics*, Vol. 11, No. 4, 2017, pp 527-534.
- Kidybinski A., Bursting liability indices of coal, *International Journal of Rock Mechanics and Mining Sciences & Geomechanics Abstracts*, Vol. 18, No. 2, 1981, pp 295-304.
- Li X. B., Gong F. Q., Wang S. F., Li D. Y., Tao M., Zhou J., Huang L. Q., Ma C. D., Du K., Feng F., Coupled static-dynamic loading mechanical mechanism and dynamic criterion of rockburst in deep hard rock mines, *Chinese Journal of Rock Mechanics and Engineering*, Vol. 38, No. 4, 2019, pp 708-723.
- Li Z. Y., Wu G., Huang T. Z., Liu Y., Variation of energy and criteria for strength failure of shale under triaxial cyclic loading, *Chinese Journal of Rock Mechanics and Engineering*, Vol. 37, No. 3, 2018, pp 662-670.
- Ma T. H., Tang C. A., Tang L. X., Zhang W. D., Wang L., Rockburst characteristics and microseismic monitoring of deep-buried tunnels for Jinping II Hydropower Station, *Tunnelling and Underground Space Technology*, Vol. 49, 2015, pp 345-368.
- Mitri H., FE modelling of mining-induced energy release and storage rates, *Journal South African Institute of Mining and Metallurgy*, Vol. 99, No. 2, 1999, pp 103-110.
- Qiu S. L., Feng X. T., Jiang Q., Zhang C. Q., A novel numerical index for estimating strainburst vulnerability in deep tunnels, *Chinese Journal of Rock Mechanics and Engineering*, Vol. 33, No. 10, 2014, pp 2007-2017.
- Qiu S. L., Feng X. T., Zhang C. Q., Wu W. P., Development and validation of rockburst vulnerability index (RVI) in deep hard rock tunnels, *Chinese Journal of Rock Mechanics and Engineering*, Vol. 30, No. 6, 2011, pp 1126-1141.
- Reddy N., Spottiswoode S. M., The influence of geology on a simulated rockburst, *Journal of the South African Institute of Mining and Metallurgy*, Vol. 101, No. 5, 2001, pp 267-272.
- Ren Y., Cao H., Yao F. C., Lu M. H., Yang Z. F., Li X. M., Review of rock brittleness evaluation methods, *Oil Geophysical Prospecting*, Vol. 53, No. 4, 2018, pp 875-886.
- Roohollah S. F., Abbas T., Long-term prediction of rockburst hazard in deep underground openings using three robust data mining techniques, *Engineering with Computers*, Vol. 35, No. 9, 2018, pp 659-675.
- Russnes B. F., Analyses of rockburst in tunnels in valley sides. Trondheim: Norwegian Institute of Technology, 1974.
- Ryder J. A., Excess shear stress in the assessment of geologically hazardous situations, *Journal South African Institute of Mining and Metallurgy*, Vol. 88, No. 1, 1988, pp 27-39.
- Shang Y. J., Zhang J. J., Fu B. J., Analysis of three parameters for strain mode rockburst and expression of rockburst potential, *Chinese Journal of Rock Mechanics and Engineering*, Vol. 32, No. 8, 2013, pp 1520-1527.
- Shi C., Chu W. J., Zheng W. T., 2016. *Block discrete element numerical simulation technology and engineering application*. Beijing: China Architecture and Building Press.
- Su G. S., 2006. *Study on stability analysis and intelligent optimization for large underground caverns under high geostress condition*. Wuhan: Graduate University of Chinese Academy of Sciences.
- Su G. S., Chen Z. Y., Jiang J. Q., Mo J. H., Shi Y. J., Experimental study on energy dissipating characteristics of rockburst fragments under different loading rates, *Chinese Journal of Geotechnical Engineering*, Vol. 38, No. 8, 2016, pp 1481-1488.
- Su G. S., Jiang J. Q., Zhai S. B., Zhang G. L., Influence of tunnel axis stress on strainburst: an experimental study, *Rock Mechanics and Rock Engineering*, Vol. 50, 2017, pp 1551-1567.
- Wang Y. H., Li W. D., Li Q. G., Xu T., Tan G. H., Method of fuzzy comprehensive evaluations for rockburst prediction, *Chinese Journal of Rock Mechanics and Engineering*, Vol. 17, No. 5, 1998, pp 15-23.
- Wei X. J., Chen T. T., Wang X., Yu X. F., Zhou L. Y., Progress in research of the rockburst hazard, *Modern Tunnelling Technology*, Vol. 57, No. 2, 2020, pp 1-12.
- Wiles T. D., Correlation between local energy release density observed bursting conditions at Creighton Mine. Sudbury, Canada: Mines Research, 1998.
- Wu F. Y., He C., Wang B., Zhang J. B., Meng W., Liu J. S., Study on the classification of rockburst intensity of Lasa-Linzhi Railway based on stress criterion, *Journal of Southwest Jiaotong University*, Vol. 56, No. 4, 2021, pp 792-803.
- Wu Q. B., Application of microgravity method in rockburst prediction, *Progress in Geophysics*, Vol. 8, No. 3, 1993, pp 136-142.
- Xie H. P., Ju Y., Li L. Y., Criteria for strength and structural failure of rocks based on energy dissipation release principles, *Chinese Journal of Rock Mechanics and Engineering*, Vol. 24, No. 17, 2005, pp 3003-3010.
- Xu B., Xie H. P., Tu Y. J., Numerical simulation of rockburst stress state during excavation of underground powerhouse of Pubugou Hydropower Station, *Chinese Journal of Rock Mechanics and Engineering*, Vol. 26, No. S1, 2007, pp 2894-2900.
- Xu L. S., Wang L. S., Study on the laws of rockburst and its forecasting in the tunnel of Erlang Mountain road, *Chinese*

- Journal of Geotechnical Engineering*, Vol. 21, No. 5, 1999, pp 569-572.
- Yi W., Wang M., Yu D. S., Han J. J., Zhang J. T., Prediction of rock mass integrity of regional slope considering the formation lithology and geological structure, *Journal of Chongqing Jiaotong University (Natural Science)*, Vol. 37, No. 5, 2018, pp 60-64.
- Zhang C. Q., Feng X. T., Zhou H., Qiu S. L., Wu W. P., Case histories of four extremely intense rockbursts in deep tunnels, *Rock Mechanics and Rock Engineering*, Vol. 45, No. 3, 2012, pp 275-288.
- Zhang C. Q., Lu J. J., Chen J., Zhou H., Yang F. J., Discussion on rockburst proneness indexes and their relation. *Rock and Soil Mechanics*, Vol. 38, No. 5, 2017, pp 1397-1404.
- Zhang J. J., Fu B. J., Rockburst and its criteria and control, *Chinese Journal of Rock Mechanics and Engineering*, Vol. 27, No. 10, 2008, pp 2034-2042.
- Zhang S. C., Ma T. H., Tang C. A., Jia P., Wang Y. C., Microseismic monitoring and experimental study on mechanism of delayed rockburst in deep-buried tunnels, *Rock Mechanics and Rock Engineering*, Vol. 53, No. 6, 2020, pp 2771-2788.
- Zhang Y. B., Yang Z., Yao X. L., Experimental study on real-time early warning method of tunnel rock burst based on infrared radiation spatial and temporal evolutions, *Journal of Mining and Safety Engineering*, Vol. 35, No. 2, 2018, pp 299-307.
- Zhou H., Chen S. K., Zhang G. Z., Wang H. L., He H. D., Feng J., Rockburst prediction in deep lying and long tunnel based on efficiency coefficient method and ground stress filed inversion, *Journal of Engineering Geology*, Vol. 34, No. 2, 2020, pp 1-11.
- Zhou H., Yang F. J., Zhang C. Q., Lu J. J., 2015. *Methods for numerical simulation and evaluation of rock burst and rock burst*. Beijing: Science Press.